O. Powder-Metal Performance Modeling of Automotive Components (AMD 410[i])

Project Manager: Mark Osborne
Group Leader - Materials Engineering
GM Powertrain
823 Joslyn Ave
Pontiac, MI 48340
(248) 255-6200; fax: (248) 857-4425; e-mail: mark.osborne@gm.com

Principal Investigator: Mark F. Horstemeyer (Paul T. Wang, Youssef Hammi)
CAVS Chair in Solid Mechanics & Professor, Mechanical Engineering
Mississippi State University
206 Carpenter Bldg., P.O. Box ME
Mississippi State, MS 39762
(662) 325-7308; fax: (662) 325-7223; e-mail :mfhorst@me.msstate.edu

Russell A. Chernenkoff (retired, Ford Motor Company)
Metaldyne Sintered Components
47603 Halyard Drive
Plymouth, MI 48170-2429
(734) 582-6227; fax : (734) 582-6250; e-mail: russellchernenkoff@metaldyne.com

Jean Lynn, Senior Specialist
DaimlerChrysler
800 Chrysler Drive, CIMS 482-00-15
Auburn, MI 48326
(248) 512-4851; fax: (248) 576-7490; e-mail: JCL6@daimlerchrysler.com

Howard Sanderow, President (CPMT Rep)
Management & Engineering Technologies (MET)
161 Copperfield Drive
Dayton, OH 45415
(937) 832-1583, fax: (937) 832-0858; e-mail: metgroup@earthlink.net

Technology Area Development Manager: Joseph A. Carpenter
(202) 586-1022; fax: (202) 586-1600; e-mail: joseph.carpenter@ee.doe.gov

Expert Technical Monitor: Philip S. Sklad
(865) 574-5069; fax: (865) 576-4963; e-mail: skladps@ornl.gov

---

Contractor: U.S. Automotive Materials Partnership
Contract No.: FC-26-02OR22910

Objective

- Develop and evaluate math-based models for powder-metallurgy component design and performance prediction. An existing USAMP microstructure-property model for castings will be extended to powder metallurgy (P/M) for practical application in low strain-rate (design and durability) and high strain-rate (toughness-driven impact

strength) environments. This model will be utilized to evaluate and optimize two component designs (a main bearing cap and a gear) as affected by material (ferrous and non-ferrous) and manufacturing processes (compaction and sintering), and will accommodate a company's analytical codes (initially ABAQUS, then other codes such as LS-Dyna, Ansys, etc.). The flexibility of this model will facilitate the evaluation of lightweight materials (such as aluminum and titanium) for future component applications.

Approach

- Determine current powder-metallurgy standards publications, component design guidelines, manufacturing, and evaluation methodologies. Provide a selection of metal powders that can satisfy design performance requirements, component design guidelines, and manufacturing and testing specifications across industry participants (Task 1).
- Evaluate and develop numerical modeling techniques to predict mechanical properties throughout P/M component sections. The transition of current materials and designs to process structural automotive P/M components creates the need to predict the properties of the component in all sections of the design. In addition, there is the necessity to provide the least-cost, lowest-mass product designs and reduced development lead-time. Adapt and/or re-develop existing math-based models which are capable of accurately predicting P/M component structures and properties throughout the compaction and sintering processes (section size, density variation, dimensional tolerances, potential for cracking), alloys and process parameters (machine functions, tool and powder temperatures, strain-rate, friction and pressure). Capture the history of a P/M part through its pressing, sintering, and life-cycle performance history using the developed multiscale methodology. (Task 2).
- Develop component- and vehicle-level testing to validate durability, quality control and performance of P/M automotive parts. Quality control for P/M parts production involves several process factors such as powder properties, press settings, tooling design, and furnace condition. Determine these process factors in terms of their impact on process variations and quality improvement. Use optimization and statistical techniques to help determine the main factors affecting the final component. Perform validation experiments in which actual boundary conditions from real processes will be used to fracture the components. This will ensure understanding of the quality effects on the product along with the modeling effort. (Task 3).
- Manage and report program activities. The proper execution of this task will greatly enhance the value of the overall program. The types of reports and guidelines generated from this program, i.e., will be in accordance with DOE and USCAR requirements. (Task 4).
- Perform technology/commercial transfer throughout the automotive value chain: Unlike aluminum, plastics and steel, there are no major R&D/technical institutions fostering the necessary infrastructure to support the large-scale application of automotive P/M components. For this reason, if the auto industry wishes to take advantage of P/M's potential weight and cost-reduction opportunities, nurturing through programs sponsored and directed by USCAR will be required. The project team will request the professional support of societies to publish notices of meetings and project information, as released by the project team. (Task 5).

Accomplishments

- Compaction of TR bars and cylindrical samples at different densities for three different powders.
- Compaction Modeling Status: Simulation of cylindrical samples and comparison with compaction data.
- Ongoing material characterization of the FC-0205 Ancorsteel powder provided by Hoeganaes.
- Compaction validation experiments at Cincinnati, Inc. to support the modeling effort.
- Sintering Modeling Status: Development of algorithm for implementation into ABAQUS/Standard.
- Establishment of a partnership with Metaldyne, LLC for the optimization of P/M automotive parts.

Future Direction

- Continue the microstructural evaluations and mechanical property tests on P/M cylinder geometry to determine microstructure-property relations during compaction, sintering, and in-service duty life. With the above software developed, the model will be correlated to these microstructure-property relations.
- Develop die compaction of cylindrical specimens using cylindrical dies with holes of different diameters to replace the triaxial compaction tests, and determine the cap surface plots.
- Determine the interparticle friction coefficient, using a simple Coulomb law of friction, by measuring the tangential forces at the contact surface, and determine the influencing parameters contributing to the friction effects.
- Develop the expression of the tangent matrix $\Delta\sigma/\Delta\varepsilon$ to implement the developed compaction model into the finite element code ABAQUS/Standard to predict the springback of compacted parts during ejection.
- Implement the sintering model in ABAQUS/Standard.
- Predict the material state during the powder compaction and sintering processes with the developed math-based models for a main bearing cap provided by Metaldyne, LLC.
- Measure the density of each piece of parts compacted at Cincinnati, Inc. by means of Archimedes' principle and hardness testing, and compare the results with modeling.
- Perform tension, compression, torsion and fatigue tests on material samples provided by Metaldyne
- Validate the process model (including tool geometry, friction, tool and metal temperatures, and pressure) and property models on the P/M bearing cap and gear with experiments, in collaboration with the partner Metaldyne.
- Work in collaboration with Chaman Hall (Metal Powder Products – MPP) on lightweight materials such as aluminum for the bearing cap.
- Explore the possibility of using an adaptive meshing procedure with CUBIT software developed at Sandia National Laboratories to model the powder flow during compaction and avoid mesh distorsion.
- Explore the DEM software provided by the USACE Engineer Research and Development Center (ERDC) to study die filling and powder transfer, to determine the density distribution before compaction.

Introduction

The Powder Metallurgy Performance project started in October 2004 at the Center for Advanced Vehicular Systems (CAVS) with guidance from the Big Three automakers (General Motors, Ford, and DaimlerChrysler) and the Center for Powder Metallurgy Technology of North America (CPMT). After the literature review and the establishment of a test matrix during the first year, the major accomplishments during this second year were (i) the run of closed-die compaction at different densities of TR bars and cylindrical samples necessary for the material characterization, and simple-shape parts on a Cincinnati. Inc. press for the validation of our model; and (ii) the validation of the P/M compaction constitutive model that was implemented in ABAQUS/Explicit. In the second year, the ongoing activities are (1) the development of a stress integration algorithm to implement the sintering model in ABAQUS/Standard, (2) the characterization of the FC-0205 powder, and (3) quantification of powder compaction data on simple-shape green parts pressed at Cincinnati, Inc.

Powder Characterization

Several experiments were conducted on the FC-0205 steel-based powder provided by Hoeganaes for the microstructural characterization and mechanical property determination. Three variants of the FC-0205 were considered in this work; the two first powders contain different percentages of Acrawax (0.6% and 1.0%), and the third powder was used at Cincinnati to run compaction tests (with 0.6% lubricant). These three powders were denominated powder I, II and III respectively. A large quantity of green samples were compacted at Penn State University and then analyzed at CAVS using different equipment such as SEM, optical

microscope, X-ray computed tomography (CT), etc. These experiments are part of the ongoing modeling effort to determine the model parameters and quantify the microstructure.

Table 1. Average density and dimension of green round and TRB specimens.

Round Specimen – 1.25 inch diameter (5 samples per density – Total: 90 samples)					
Average Density (g/cc)			Average Height (inch)		
I	II	III	I	II	III
6.58	6.61	6.63	0.7623	0.7461	0.7432
6.61	6.69	6.77	0.3753	0.3709	0.3629
6.59	6.69	6.77	0.2003	0.1989	0.1986
7.18	7.06	7.19	0.7891	0.7986	0.7824
7.17	7.06	7.17	0.4513	0.4506	0.4438
7.09	7.05	7.15	0.2364	0.2363	0.2360
TRB specimen – 0.50 inch thick (5 samples per density – Total: 120 samples)					
Average Density (g/cc)			Average Thickness (inch)		
I	II	III	I	II	III
5.93	5.98	5.92	0.4889	0.4833	0.4868
5.75	5.81	5.72	0.4779	0.4722	0.4789
6.08	6.12	6.10	0.4994	0.4916	0.4926
6.30	6.32	6.30	0.4998	0.4962	0.4962
6.54	6.52	6.52	0.4953	0.5001	0.4972
6.82	6.81	6.81	0.5015	0.4998	0.4990
7.01	7.02	7.10	0.5026	0.4973	0.4913
7.33	7.10	7.22	0.4932	0.5066	0.5004
TRB specimen – 0.25 inch thick (20 samples per density – Total: 540 samples)					
Average Density (g/cc)			Average Thickness (inch)		
I	II	III	I	II	III
5.63	5.65	5.61	0.2509	0.2470	0.2496
5.83	5.81	5.80	0.2501	0.2481	0.2487
6.09	6.06	6.04	0.2464	0.2446	0.2468
6.29	6.31	6.32	0.2488	0.2445	0.2457
6.42	6.46	6.45	0.2495	0.2450	0.2475
6.63	6.66	6.58	0.2490	0.2461	0.2486
6.81	6.84	6.87	0.2487	0.2471	0.2467
7.06	6.97	7.02	0.2495	0.2487	0.2480
7.19	7.08	7.30	0.2498	0.2507	0.2415

Compaction of green compact samples

Using a 60-ton Gasbarre press at Penn State University, round and transverse rupture bar (TRB) specimens were compacted at different densities (Table 1). The press is equipped with several sensors to record the force of the lower and upper punches, and also the displacement of the upper punch and the die plate for each sample. Because the powder was fed manually using a simple shoe, a slight variation in density from one sample to another was observed. To obtain the desired density and thickness for each series, a trial-and-error method was applied by adjusting manually the tonnage and the fill depth.

Densities and dimensional measurements for 1.25-inch-diameter round specimens were made at Penn State using a caliper (0.0005”) and a lab scale (1mg). The same measurements for TRB samples were performed at CAVS using a caliper (0.0005”) to measure the length of 1.25 inch, a micrometer (0.00005”) to measure the width of 0.50 inch, and the thicknesses of either 0.50 or 0.25 inch, and a lab scale (0.1mg). All data are saved in Excel files. Press loads and displacement were plotted only for the first sample of each group.

TRB specimens will be used for powder characterization, such as green strength, sintering applications, hardness testing and X-ray CT. Round specimens will be used for a first validation and calibration of the compaction constitutive model developed at CAVS by looking at the final average density and force-displacement curves.

Cold isostatic compaction (CIP) was also conducted at Penn State University for 5 different pressures (10, 20, 30, 40 and 50 tsi). The volume of the samples still needs to be cautiously measured since certain samples were broken into several pieces.

Green Strength

Green strength was measured for TRB green samples of 0.25 in. and 0.50 in. thickness according to the MPIF Standard Method 15 for the three variants of the FC-0205 powder. The tests were performed on the three first TRB samples of each density in Table 1.

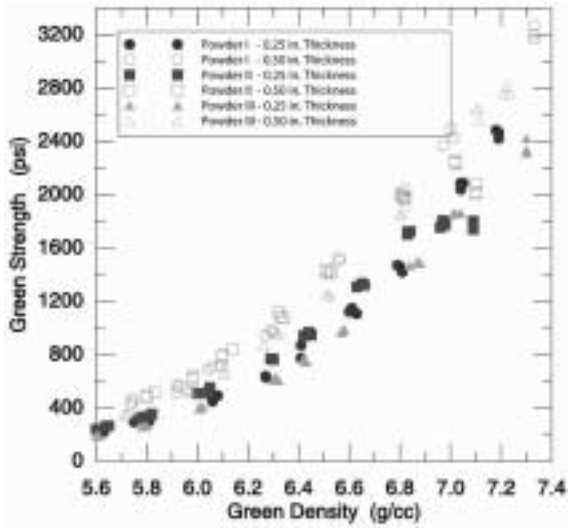

Figure 1. The effect of compaction pressure on the green strength of FC-0205 powders.

Particle shape and size distribution

A representative sample of powder was collected for the particle-size characterization analysis. In order to avoid particle agglomeration, an ultrasonic agitation was sufficiently applied to disperse the cluster of particles and assure a proper particle-size characterization. This process was repeated for every tested powder.

The particle-size analysis was achieved using a sieve analysis by following the MPIF standard method 05. Three different screens were weighed and stacked with decreasing mesh opening. A 100g powder sample was loaded on the top of the screen and agitated in a sieve-shaking device for a period of fifteen minutes. After the agitation, each screen was weighed calculating the percentage of powder sample retained or passed throughout the mesh. The particle-shape distribution was determined from a microscopic imaging method.

Tap Density

The tap density was determined using the Hall flowmeter according to the MPIF Standard Method 04, obtaining 3.13 g/cm^3. The apparent density was determined using the Hall flowmeter, obtaining 3.09 g/cm^3.

Chemical Composition

The chemical composition was determined using two different methods, an optical-emission spectrometer (OES) and an EDX mapping using a SEM.

The optical-emission spectrometer creates an arc or spark discharge vaporizing the sample, and the atoms and ions contained in the atomic vapor are excited into emission of radiation. The radiation emitted is passed to the spectrometer optics via an optical fiber, where it is dispersed into its spectral components. From the range of wavelengths emitted by each element, the most suitable line for the application is measured by means of a photomultiplier. The radiation intensity, which is proportional to the concentration of the element in the sample, is recalculated internally from a stored set of calibration curves and can be shown directly as percent concentration. This procedure was repeated 21 times using different density samples to obtain an average and accurate value.

Energy-dispersive X-ray (EDX) in the Scanning Electron Microscope (SEM) was used to identify the elemental composition of the specimen. A loose powder sample was set on conductive tape and observed under the SEM. A representative image that contained most of the powder mixture was selected as our region of interest. From this method the location of the major alloying components like carbon and copper in the region of interest selected before, were obtained using the EDX spectrum that shows the energy level received for each element. The element weight percentage of a selected powder sample was also determined.

Figure 2 shows the dispersion of the elements in the FC-0205 iron powder (only a sample from the first powder was analyzed).

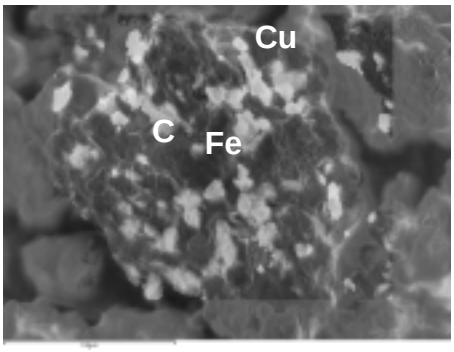

Figure 2. Mix of all major compounds in the iron powder FC-0205.

Microstructural Features

The TRB samples were cold mounted in order to separate the "pull-out" artificial pores from the true pores. The specimens were ground and polished according to standard practices. The etchant used for the examination of the microstructure was 2 % nital. The sample preparation was performed following standard procedures to preserve the pores and grain structures.

The grain-size distribution (Table 2) was obtained using an intercept procedure. The grain size is determined by the number of times a test line cuts across, or is tangent to, grain boundaries.

Table 2. Grain Size number for the green compacted samples at 6.8 g/cc.

Compacted Density g/cc	Grain Size No. G	Grains/ unit area	Average Grain Area	Average Diameter
		No./in at 100x	μm^2	μm^2
6.8	7.50	90.51	7.13	26.7

All six sides of the TRB sample were analyzed to obtain an average grain-size number (G) for each density.

An image analyzer software developed at CAVS was used to measure the porosity, pore nearest neighbor and the pore volume fraction. Microstructure images were taken in an optical microscope at a 100 µm resolution for each density and each side of the TRB samples. The software calculates and highlights the pore area, the minimum, mean and maximum first nearest neighbor. Further calculations are necessary to calculate the porosity and the pore volume fraction.

The images for the 7.0 g/cc and 7.2 g/cc green samples that have been taken are getting processed to obtain the values of Table 2.

X-ray CT

For crack detection and density measurement, CAVS facilities recently acquired a Phoenix V/Tome/X Computed Tomography system with the 225D directional target tube and the 160NF transmission target tube.

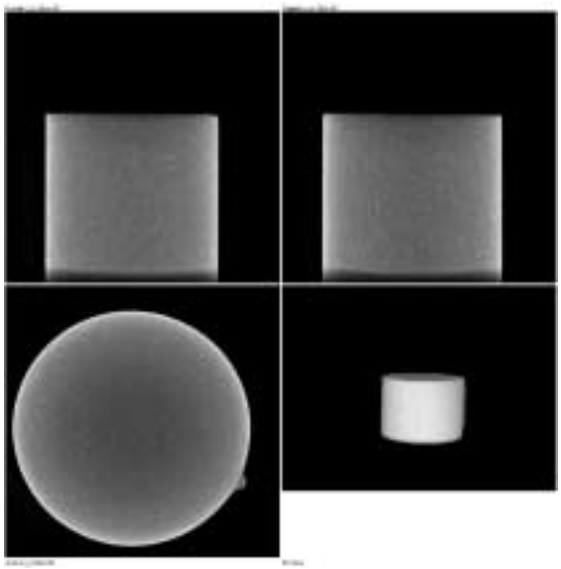

Figure 3. CT scans of 9-mm-diameter compacted samples after being machined.

Figure 3 shows the reconstruction of the density distribution of 9-mm-diameter round samples of different known densities. The samples were scanned using the same scanning conditions (beam current and voltage). Two copper filters of one millimeter thickness were used to avoid beam hardening artifacts. The attenuation of the X-rays was measured by an array of detectors over many views (X-ray paths) by stacking contiguous two-dimensional images and mathematically reconstructing them into 2D or 3D.

Quantitative interpretation of reconstructed CT images in terms of the mass density or the composition of the object usually is done by

assuming an attenuation that is linearly dependent on the mass density or material thickness, especially in dense materials. However, this is only true for monochromatic sources [Van de Casteele et al., 2002]. As with most of the CT systems, the V/Tome/X CT system uses polychromatic X-ray sources, which can produce significant artifacts in the reconstructed image due to non-linearities. This makes the translation of the CT values inexact or not possible at this time. CAVS is looking currently for a solution to overcome the complexity of the projection data and eliminate statistical noise artifacts. Different methods currently exist to minimize these artifacts. A method for compensating non-linearities divides the detected spectrum into a low- and high-energy region, and the resultant signals are processed to obtain a photoelectric component and a Compton scattering component [Macovski et al., 1976]. Another commonly-applied correction method is based on a linearization procedure where the measured nonlinear relationship is fitted with polynomials [Van de Casteele et al. 2002].

Validation of Simple Compaction Parts

As part of the CAVS modeling effort, CPMT and CAVS conducted a validation trial of a multi-level P/M part (Figure 4) at Cincinnati, Inc. with the help of Kenneth Cradler and two other assistants, all three are employees of Cincinnati, Inc. The goal of this trial was to validate the powder-compaction model in terms of the density distribution, the powder transfer during compaction, and the fracture mechanism during the ejection process.

The FC-0205 powder III was used and the apparent density value was measured at 3.29 g/cc during these runs. The parts fell into 3 groups based on overall average density (6.45, 6.80 or 7.10 g/cc). The trials were conducted by varying the fill depth of each column, initially with an even ratio of compaction in each column, and then by adding or reducing the amount of fill (powder) above the lower punch by re-positioning it. This changes the amount of powder to be compacted and, therefore, affects compaction response. The pressure remained the same but the density achieved changed (Table 3). The columns 1, 2, 3 and 4 correspond respectively to the heights 0.870 in., 0.475 in., 1.000 in., and 0.510 in Figure 4.

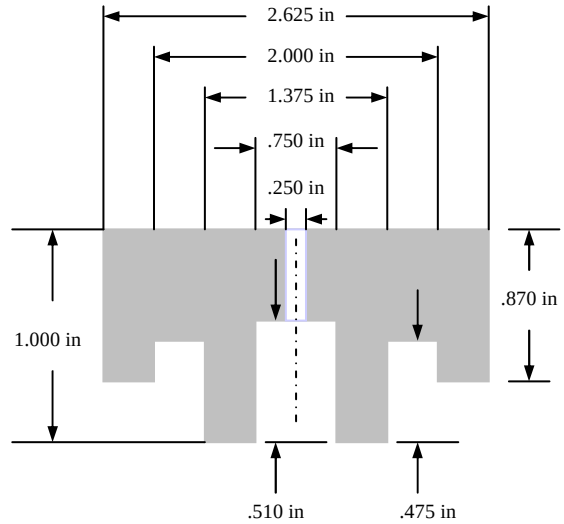

Figure 4. Drawing of the Cincinnati Inc. sample part.

The pressing condition of the upper punch (overall press tonnage) and all press platen motions, in terms of displacement versus time, were obtained and recorded through the data acquisition system (DAS) and are available through the Windaq software. Measurements were taken using displacement sensors attached to each platen with individual data points acquired about every 100 milliseconds. These data will be used in a finite-element input file as boundary conditions.

After ejection, cracks were observed in the series where the powder fills were modified by a decrease in column 1 and an increase in column 3 (series 3 and 5 in Table 3). Parts were ejected with no apparent crack in the series where each column depth was filled with an even ratio of compaction (Series 1, 4 and 7). No apparent crack was observed in series 6 also, where the test transferred powder from column 1 and added it to column 2.

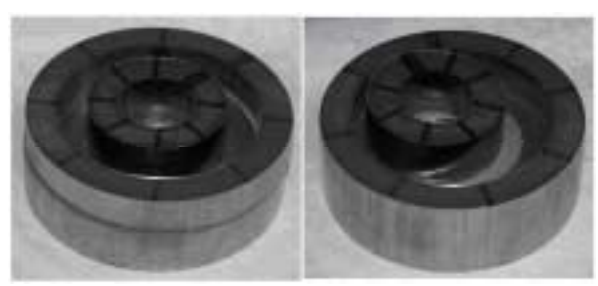

(a) (b)

Figure 5. (a) Crack in the skirt region after ejection. (b) Crack in the center hub after ejection.

In series 3, the amount of powder transferred from column 3 to column 1 did not actually occur if the density was to be equalized during compaction. As a consequence, a crack was seen in the skirt (lower portion) region of column 1 at the step between column 1 and column 2 powder heights (Figure 5). We believed the low green strength at this density may have also been a contributing factor. In series 5, the test changed the powder fills by reducing the fill in column 1 and increasing the fill in column 3 to compensate so the overall part density remained at 6.80 g/cc. Due to the extensive transfer of powder, the parts cracked in the skirt region (Figure 5a) or in the center hub (Figure 5b), depending on the press motions and compensating air pressure. Ten pieces were run in each mode.

Table 3. Cincinnati, Inc., Test Runs.

Series #	Samples	Average Density g/cc	Fill Position Column 1, in.	Fill Position Column 2, in.	Fill Position Column 3, in.	Fill Position Column 4, in.
1	10	6.45	1.644	1.017	1.943	0.809
2	10	6.45	1.675	1.020	1.821	0.809
3	10	6.45	1.594	1.027	2.157	0.809
4	11	6.80	1.762	1.064	2.027	0.809
5	20	6.80	1.649	1.064	2.229	0.809
6	10	6.80	1.569	1.298	1.952	0.809
7	10	7.10	1.863	1.153	2.093	0.809

The action items performed to post-process the 81 samples pressed at Cincinnati are:
1) measurement of the part pressing lengths in eight evenly spaced locations, i.e., every 45 degrees around the circumference; 2) measurement of the part diameter dimensions (five values) in the as-pressed condition; and 3) sectioning each individual part into many pieces (only 3 parts from each set). Sections were made in the vertical and horizontal planes. A band saw was recently purchased at CAVS to perform the cutting between columns. The goal of this sectioning is to produce a very accurate density map measuring the sectional density of the parts by the immersion method (Archimede's principle). X-ray tomography mapping and micro-hardness testing will also be conducted on some other parts from each set. The remaining parts will be used for the sintering experiments to measure the shrinkage and the dimensional changes.

Constitutive Modeling of Compaction

The finite-element method is an efficient numerical tool to improve the fundamental understanding of the mechanics of compaction and to develop appropriate constitutive laws in terms of the evolution of suitable state variables for the full range of possible compaction mechanisms. It is a complementary technique to characterize the material parameters when measured data are not consistent from a testing point of view [Sinka et al.,2001.]. By using the inverse method to match the experimental results, the finite-element method can provide a consistent calibration of material parameters.

After the development of the implementation of a constitutive model for powder compaction based on a Modified Drucker/Prager Cap model, which was implemented in ABAQUS/Explicit via the user material subroutine VUMAT, three simulations describing closed-die compaction of cylindrical parts were performed to validate the model. The numerical results were compared to three round samples compacted at Penn State University of final average densities 7.17 g/cc, 7.14 g/cc and 7.20 g/cc using powder III, and of respective final heights 0.2405 in., 0.4445 in. and 0.7780 in. (see above section). Simulations were made using axisymmetric elements (CAX4R with reduced integration) and a symmetry plane was assumed; therefore, only a quarter of the part was meshed. In this comparison between numerical results and experimental data, we looked at the force-displacement of the upper punch and the density distribution, which was compared to the final average density of compacted samples.

Because not all of the density-dependent parameters were able to be characterized, such as the evolution

of the interparticle friction, the cohesion, the cap eccentricity, and the elastic properties, some data were used from the literature [Coube and Riedel, 2001; Wikman, 2001].

In the literature, people found that the die-wall friction is a function of the powder density. The measured friction coefficients range from about 0.2 at high densities to 0.8 or even higher at low densities [Wilkman, 2001, Coube and Riedel, 2001]. Therefore, the die-wall friction is also chosen as constant and its value is μ=0.2 throughout the analysis (which corresponds to the friction value when the force applied to the punch is very high). For the Young's modulus, its evolution is exponential with the density [Pavier and Doremus, 1999]. Here we assumed that the Young's modulus value at full density (7.85g/cc) should be equal to that of a dense steel material, which is 200 GPa.

The tap density provided by the supplier (3.02 g/cc) and the final density were used to estimate the initial fill depth and the course of upper punch assuming there is no die deflection.

Figure 6 shows the density distribution of the three samples at the end of the simulation. We can observe the gradient of density along the die wall due to the friction. In the center of the part, the densities are homogeneous and the density values are very close to the average measured densities, which are 7.17 g/cc, 7.14 g/cc and 7.20 g/cc, respectively, for the round samples of height 0.20 in., 0.40 in., and 0.80 in.

In Figure 7, the predicted evolution of the force displacement is compared to experimental data. There is a good agreement for the maximum force value, but the values differ when the force is increasing. This difference is due to the material parameters of the cap hardening, which need to be optimized for a better agreement.

(a) Round specimen of height 0.8 inches.

(b) Round specimen of height 0.4 inches.

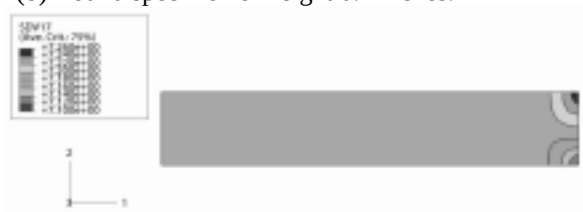

(c) Round specimen of height 0.2 inches.

Figure 6. Density distribution for the round cylinders of final height after compaction.

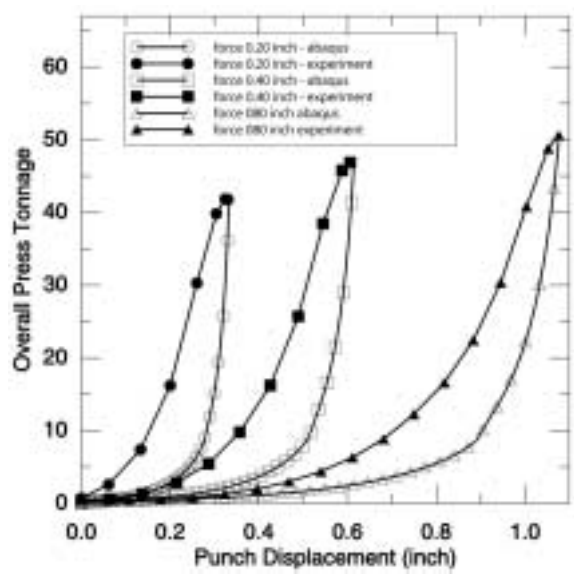

Figure 7. Comparison of the punch force-displacement for the round cylinders of final height 0.20, 0.40 and 0.80 inches.

Figure 8. 3D Density distribution for the round cylinder (0.2 inch final height).

Comparison of Axisymmetric vs. 3D.

The implementation in ABAQUS/Explicit via the user subroutine VUMAT has been done such as it can be generally used for any 3D, plane strain and axisymmetric applications. A closed-die compaction of a cylindrical specimen can be simulated using either 3D or axisymmetric elements. An axisymmetric analysis is much faster and requires less CPU time. A method to validate the 3D implementation is to compare it to the axysimmetric analysis for the same application. Figures 6a, 8 and 9 show a good match between the two analyses. Because the axisymmetric mesh is more refined around the outside diameter, the contour map on Figure 6a shows more contour values.

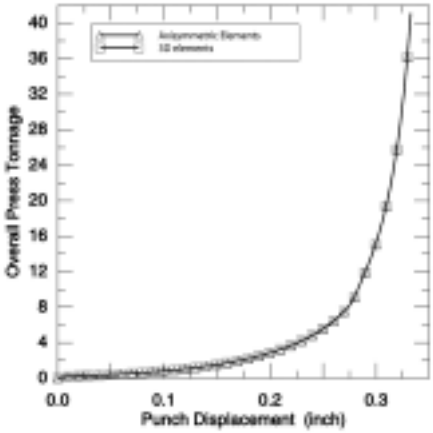

Figure 9. Comparison of the force-displacement using 3D and axisymmetric elements.

Sintering Modeling

An algorithm to implement the sintering constitutive model of Penn State University [Mckeeing and Kuhn, 1992; Olevski, 1998] in ABAQUS/Standard was developed based on the stress integration algorithm proposed by Govindarajan and Aravas [1993]. This algorithm will be implemented into the user material subroutine UMAT to facilitate the transition between the compaction and sintering processes.

Partnership with Metaldyne

In fall 2006, Metaldyne agreed to be our partner and support our modeling effort. Their contribution in this project should be:

Supply CAVS with a large number of "typical" green and sintered parts for validation studies of density distribution and measurement of mechanical and physical property.

Provide powder and test material samples for tension, compression and fatigue tests

Provide information on the process (geometry, load and tool motions) and the performance data of a bearing cap.

Conclusions

The Powder-Metallurgy Performance Modeling of Automotive Components project has mostly completed the modeling of the compaction process. Green round and TRB samples and simple parts have been made and measured for material characterization, parameter calibration and model validation. Further tests and measurements are necessary on these specimens to complete the validation of the constitutive compaction model. Using the new sintering capabilities and equipment at CAVS, these samples will also be tested for validation of the sintering model. After completion of the compaction and sintering modeling, simulations of the main bearing cap will be performed in comparison with the process and performance data provided by Metaldyne. The final objective will be the design, performance and mass optimization of the bearing cap by using lightweight materials such as aluminum and titanium.

Acknowledgements

The authors would like to acknowledge funding from the Center for Advanced Vehicular Systems at Mississippi State University and from USAMP Lightweight Materials Group. We also acknowledge valuable guidance received from William F.

Jandeska (Center for Powder Metallurgy Technology – CPMT) and Scott Burrell (DaimlerChrysler).

References

1. Abaqus, User's Manual, Version 5.8, Hibbit, Karson & Sorensen, Inc., 2003.

2. Coube, O. and Riedel, H. "Numerical Simulation of Metal Powder Die Compaction with Special Consideration of Cracking," Powder Metallurgy, Vol. 43, No. 2, 2000, pp. 123–131.

3. Govindarajan, R.M., and Aravas, N., "Deformation processing of metal powders: Part II – Hot isostatic pressing", Int. J. Mech Sci. Vol. 36, No. 4, 1994, pp. 359-372.

4. Macovski, A., Alvarez, R.E., Chan, J.L.-H., Stonestrom, J.P. and Zatz, L.M., "Energy dependent reconstruction in X-ray computerized tomography," Computers in Biology and Medicine, Vol. 6, No. 4, 1976, pp. 325–334.

5. McMeeking, R.M., and Kuhn, L.T., "A Diffusional Creep Law for Powder Compacts," Acta Metal. Mat., Vol. 40, 1992, pp. 961–969.

6. Olevsky, E. A., "Theory of Sintering: from Discrete to Continuum," Material Science & Eng.: R: Reports, Vol. 23, No. 2, 1998, pp. 41–100.

7. Pavier, E., and Doremus, P., "Triaxial characterisation of iron powder behaviour," Powder Metallurgy, Vol. 42, No. 4, 1999, pp. 345–352.

8. Sinka, I.C., Cocks, A.C.F., Morrison, C.J., and Lightfoot, A., "High pressure triaxial facility for powder compaction," Powder Metallurgy, Vol. 43, No. 3, 2000, pp. 253–262.

9. Van de Casteele, E., Van Dyck, D., Sijbers, J. and Raman, E., "An energy-based beam hardening model in Tomography," Phys. Med. Biol. Vol. 47 (2002) pp. 4181–4190.

10. Wikman, B., Solimannezhad, N., Larsson, R., Oldenburg, M., and Haggblad, H.-A., "Wall friction coefficient estimation through modelling of powder die pressing experiment," Powder Metallurgy, Vol. 43, No. 2, 2000, pp. 132–138.

[i] Denotes project 410 of the Automotive Metals Division (AMD) of the United States Automotive Materials Partnership (USAMP), one of the formal consortia of the United States Council for Automotive Research (USCAR), set up by the "Big Three" traditionally USA-based automakers to conduct joint pre-competitive research and development.